第 xx 卷第 x 期
xxxx 年 x 月

控 制 理 论 与 应 用
Control Theory & Applications

Vol. xx No. x
Xxx. xxxx

依赖方位角测量的多智能体系统事件触发协同定位

胡斌斌[1,2], 张海涛[1,2†]

(1. 华中科技大学 人工智能与自动化学院, 图像信息处理与智能控制教育部重点实验室, 湖北 武汉 430074;
2. 数字制造装备与技术国家重点实验室, 湖北 武汉 430074)

摘要: 论文提出了一种基于事件的方案来实现三维空间多智能体系统的方位定位。依赖方位角刚度设计了一种事件触发的定位方法，该方法在少数个体方位角已知的前提下，可以对集群网络中所有个体进行定位。为了保障方法的有效性，利用输入到状态的稳定原理，得到了上述闭环控制系统的稳定性条件，并且理论保证Zeno行为不发生。最后，通过二维和三维的数值仿真验证了所提出的多智能体系统事件触发定位控制方案的有效性。

关键词: 定位; 方位角刚度; 事件驱动控制; 多智能体系统

引用格式: 胡斌斌, 张海涛. 控制理论与应用论文格式要求. 控制理论与应用, 2021, 38(x): 1 – 10

DOI: 10.7641/CTA.2021.10766

Bearing-based Localization of Multi-Agent System with Event-Triggered Strategy

HU Bin-Bin[1,2], ZHANG Hai-Tao[1,2 †]

(1. Key Laboratory of Image Processing and Intelligent Control, School of Artificial Intelligence and Automation, Huazhong University of Science and Technology, Wuhan 430074, China;
2. State Key Lab of Digital Manufacturing Equipment and Technology, Wuhan 430074, China.)

Abstract: This paper develops an event-based scheme to attain bearing-based localization of multi-agent system in arbitrary dimension. Essentially, an event-triggered localization law is designed accordingly to the bearing rigidity, which is to localize all the agents in a static network given the bearings of a subset of agents. The conditions guaranteeing asymptotically stability of the closed-loop MAS governed by the proposed controller are derived with the assistance of input-to-state stable (ISS) principle. Significantly, Zeno behavior is excluded as well. Finally, 2-D and 3-D numerical simulations are conducted to substantiate the effectiveness of the proposed event-triggered localization control scheme.

Key words: Localization; bearing rigidity; event-triggered control; multi-agent system

Citation: HU Bin-Bin, ZHANG Hai-Tao. Bearing-based Localization of Multi-Agent System with Event-Triggered Strategy. *Control Theory & Applications*, 2021, 38(x): 1 – 10

1 Introduction

In recent years, collective control of the multi-agent systems (MASs) has attracted more and more attention due to its extensive applications in multi-robot collaboration, multiple unmanned system localization, wireless sensor network optimization, and so on [1–14]. Taking the localization control of the networked system for example, the localization technology is indispensable for smuggling detection, contour mapping, environment surveillance, resources exploration, etc.

The objective of MAS localization is to localize all the agents in a static network with the assistance of the locations of a subset agents and inter-neighbor relative measurements. According to the types of measurements utilized in the localization, the existing works can be classified into position-based [15–17], distance-based [18–21] and bearing-based strategies [22–25].

Due to the associated theoretical challenges, initial efforts are devoted to the methods according to positions and distances [15–21], which are however heavily costly due to the high-accuracy binocular vision sensors and GPS devices. Moreover, in modern complex collective missions like aquatic resource exploration of multi-unmanned surface vessels (USVs), efficient and precise position / distance sensors may not be always available, which intensifies the challenges in localization control. As a remedy, the bearing information (i.e., bearing vectors or angles) only requires less costly onboard bear-

Received 21 August 2021; accepted: 10 December 2021.
†Corresponding author. E-mail: zht@mail.hust.edu.cn; Tel.: +86 27-87558443.
Recommended by Associate Editor. HONG Yiguang
Supported by the National Natural Science Foundation of China (51729501, U1713203, 61803166) and the National Natural Science Foundation of Hubei Province (2019CFA005).

ing sensors such as the pin-hole cameras and wireless sensor arrays [26], which is desirable in modern large-scale applications to fulfill more and more complex marine missions. Therefore, it becomes an urgent tendency to develop a more practical and economic localization control scheme of the MASs merely based on relative bearing measurements.

In localization control techniques with bearing-based measurements, one of the main challenges lies in the nonlinearity of the bearing controllers, and hence the early stage works only focused on subtended bearing angles. As one of the pioneer works, Basiri & Bishop [27] proposed a bearing-only control scheme which governs three mobile agents to form localization with evenly-distributed angular phases. Zhao & Lin [28] designed a bearing-only protocol to form a cyclic localization with angular constraints. Eren & Tolga [29] developed a pattern controller for the localization of robots and sensor networks. However, such subtended bearing-based control protocols [27–29] still lack flexibility due to the invariant angles in agent's local coordinates, which thereby hinders their further applications. Afterwards, another research line of bearing rigidity emerged, which achieves a specified localization by setting desired bearing vectors with local calculation. In this pursuit, Franchi *et al.* [30] initially studied the concept of bearing rigidity. Zhao & Zelazo [31] designed a nonlinear distributed bearing-only controller without a global orientation. This scheme was afterwards [32] generalized to a protocol to form translational and scaling localizations considering external disturbances, input saturations, and collision avoidance, simultaneously. Following this research line, Tron & Thomas [33] developed a gradient-decent optimization control law to minimize the localization error and control cost of the bearing-only schemes. However, due to the increasingly pattern complexity to fulfill specific localization missions in real applications, more recent efforts have been devoted to bearing-only localization control for high-order MASs. As representive works, Zhao *et al.* firstly revealed necessary-sufficient conditions for network localizability with rigidity theoretic interpretations [34] and then designed a novel bearing-only control law to attain localization with a variety of agent dynamics including single-integrator, double-integrator, and unicycle models [35].

So far, most of the existing bearing-only localization studies [22–35] just focused on the time-driven methods, which may not be suitable due to the widely-used embedded microprocessors with limited calculation resources. Moreover, data transmissions of currently available communication capability of bearing sensors further limit the applications to large-scale localization missions. As a remedy, event-triggered schemes [36–37] have attracted more and more attention, whose core idea is to trigger the controller only when a local measurement error exceeds a threshold. An event-triggered scheme basically consists of two elements, i.e., a distributed controller to govern each agent, and a triggering function determining what time to be updated [38–42]. Compared with time-driven methods, event-triggered schemes could reduce calculation, communication and sampling cost whereas maintaining satisfactory control performances. However, due to the theoretical challenges in synthesizing the bearing input saturation constraints of bearing rigidity and event-based dynamics, so far few efforts have been devoted to the event-triggered localization control with bearing rigidity. That naturally motivates us to develop a niche event-triggered bearing-only localization controller.

As an initial exploration of bearing-based MAS localization control with event-triggered techniques, the main contribution of this paper is to propose an event-triggered bearing-only controller to localize all the agents in arbitrary dimensions, where the Zeno behaviors [36] are theoretically guaranteed to be excluded in the proposed framework.

The remainder of this paper is organized as follows: Section II presents problem formulation. Section III develops an event-triggered scheme for bearing-based localization. Moreover, the conditions are derived to guarantee both the closed-loop stability and the Zeno-free feature in the same section. Afterwards, numerical simulation are conducted to substantiate the effectiveness of the proposed method in Section IV. Conclusions are finally drawn in Section V.

Throughout the paper, $\mathbb{R}, \mathbb{R}^+$ denote sets of the real and positive real numbers, respectively. $\mathbb{R}^n$ denotes the n-dimensional Euclidean Space. $\| * \|$ is the Euclidean norms, $\mathbf{1}_m := [1, \dots, 1]^\top \in \mathbb{R}^m$, $I_n \in \mathbb{R}^{n\times n}$ is the identity matrix. $\otimes$ denotes the Kronecker product, $(*)_{i,j}$ represents the (i,j)-th entry of matrix $*$, $\lambda_{\min}(*)$ denotes the smallest eigenvalue of symmetric matrix $(*)$, and $\nabla(f)$ is the gradient of a function f. Given $P_k \in \mathbb{R}^{q\times q}$ for $k = 1, \dots, m$, $\mathrm{diag}(P_k) \in \mathbb{R}^{mq\times mq}$ represents a block-diagonal matrix with diagonal entries P_1 to P_m.

2 Problem formulation

Consider a leader-follower MAS with the first l agents as the leaders, i.e., $\mathbb{I}_l := \{\nu_1, \nu_2, \dots, \nu_l\}$ and the reminder $f := n - l$ agents as the followers, i.e., $\mathbb{I}_f := \{\nu_{l+1}, \nu_{l+2}, \dots, \nu_n\}$, define $G(\nu, \boldsymbol{\varepsilon})$ as the undirected interaction topology among agents with $\nu = [\nu_1, \nu_2, \dots, \nu_n] = \mathbb{I}_l \cup \mathbb{I}_f$ the vertex set and $\boldsymbol{\varepsilon} \subseteq \nu \times \nu$ the edge set. $\mathcal{N}_i = \{j \in \nu, (i,j) \in \boldsymbol{\varepsilon}\}$ denotes the neighbors of agent i, where the connection (i,j) represents agent i has access to agent j.

Let $p_i \in \mathbb{R}^d$ be the positions of agent i with the dynamics formulated as below,

$$\dot{p}_i(t) = u_i(t), i \in \nu \tag{1}$$

with $u_i(t) \in \mathbb{R}^d$ being the control input. Suppose only bearing information is available to the agents, and define the edge vector $e_{i,j} \in \mathbb{R}^d$ for the edge (i, j) as

$$e_{i,j} := p_j - p_i, \tag{2}$$

which then leads to the bearing vector $g_{i,j} \in \mathbb{R}^d$ (see e.g., [35]) as

$$g_{i,j} := \frac{e_{i,j}}{\|e_{i,j}\|}. \tag{3}$$

Thereby, the orthogonal projection matrix $P_{i,j} \in \mathbb{R}^{d\times d}$ writes

$$P_{i,j} := I_d - g_{i,j}g_{i,j}^\intercal, \tag{4}$$

and hence the temporal derivative of $g_{i,j}$ becomes

$$\dot{g}_{i,j} = \frac{P_{g_{i,j}}}{\|e_{i,j}\|}\dot{e}_{i,j}, \tag{5}$$

which implies that

$$P_{g_{i,j}}g_{i,j} = 0, g_{i,j}^\intercal \dot{g}_{i,j} = 0, e_{i,j}^\intercal \dot{g}_{i,j} = 0. \tag{6}$$

Before deriving the control law, it is necessary to give the following definitions concerning bearing rigidity.

Definition 1 [43] (*Oriented Graph*) An oriented Graph is an undirected graph $G(\nu, \varepsilon)$ with an assignment of a direction to each edge.

Let m be the number of undirected edges in G, it can be deduced that the oriented graph contains m directed edges. Suppose the edge $(k_i, k_j), k_i, k_j \in \nu$ in G corresponds to the k-th directed edge in the oriented graph with $k \in M := \{1, \ldots, m\}$, in other words,

$$e_k := e_{k_i,k_j} = p_{k_j} - p_{k_i},\ g_k := \tfrac{e_k}{\|e_k\|}, k \in M. \tag{7}$$

Analogously, it follows from Eq. (6) that $P_{g_k}g_k = 0, g_k^\intercal \dot{g}_k = 0, e_k^\intercal \dot{g}_k = 0$.

Definition 2 [35] (*Incidence Matrix*) $H \in \mathbb{R}^{m\times n}$ is an incidence matrix of the corresponding oriented graph in Definition 1, where m rows denote the number of edges assigned with directions and n columns the number of vertexes. Let H_k be the k-th row of H, where $H_{k,i} = -1$ if vertex k_i is the tail of edge k, $H_{k,j} = 1$ if vertex k_j is the head of edge k, and all the other entries in the k-th row are zero.

Let $p(t) := [p_1^\intercal(t), p_2^\intercal(t), \ldots, p_n^\intercal(t)]^\intercal \in \mathbb{R}^{nd}$. It then follows from the incidence matrix H in Definition 2 and e_k in Eq. (7) that

$$\begin{aligned} e_k =& p_{k_j} - p_{k_i} \\ =& [0, \ldots, H_{k,i}, \ldots, H_{k,j}, \ldots, 0] \otimes I_d \cdot p \end{aligned} \tag{8}$$

Let $e := [e_1^\intercal, e_2^\intercal, \ldots, e_m^\intercal]^\intercal \in \mathbb{R}^{md}$, Eq. (8) could be rewritten in a compact form as

$$e = (H \otimes I_d)p = \bar{H}p \tag{9}$$

with $\bar{H} := H \otimes I_d \in \mathbb{R}^{md\times nd}$, $e := [e_1^\intercal, e_2^\intercal, \ldots, e_m^\intercal]^\intercal \in \mathbb{R}^{md}$ and $p(t) := [p_1^\intercal(t), p_2^\intercal(t), \ldots, p_n^\intercal(t)]^\intercal \in \mathbb{R}^{nd}$.

According to the definition of g_k in Eq. (7), one has [31]

$$\dot{g} = \frac{\partial g}{\partial e}\cdot\frac{\partial e}{\partial p}\cdot\frac{\partial p}{\partial t} = \mathrm{diag}\left(\frac{\mathrm{P_{g_k}}}{\|\mathrm{e_k}\|}\right)\cdot \bar{\mathrm{H}}\cdot\dot{\mathrm{p}} \tag{10}$$

with $g := [g_1^\intercal, g_2^\intercal, \ldots, g_m^\intercal]^\intercal$ and $\bar{H} := H \otimes I_d$ given in Eq. (9).

Let $p^*(t) := [p_1^*(t)^\intercal, p_2^*(t)^\intercal, \ldots, p_n^*(t)^\intercal] \in \mathbb{R}^{dn}$ be the desired positions of the leader-follower MAS, and one has that $(G, p^*(t))$ is a desired target localization with an undirected graph G, which fulfills the constant inter-neighbor bearing differences $\{g_{i,j}^*\}_{(i,j)\in\varepsilon}$ and the leader positions $\{p_i^*(t)\}_{i\in\mathbb{I}_l}$ with bearing-based measurements.

Next, to achieve the uniqueness of $(G, p^*(t))$, the bearing Laplacian $\mathcal{B} \in \mathbb{R}^{dn\times dn}$ stemming from [34] is then introduced with the block of submatrix as

$$\mathcal{B}_{ij} := \begin{cases} \mathbf{0}_{d\times d}, & i \neq j, (i,j) \notin \varepsilon, \\ -P_{g_{i,j}^*}, & i \neq j, (i,j) \in \varepsilon, \\ \sum_{k\in\mathcal{N}_i} P_{g_{i,k}^*}, & i = j, i \in \nu, \end{cases}$$

where $P_{g_{i,j}^*}$ is the orthogonal projection matrix with the desired bearings vector $g_{i,j}^*$.

In accordance to the definition of leader-follower MAS ($\mathbb{I}_l \cup \mathbb{I}_f$), the bearing Laplacian $\mathcal{B}$ could be partitioned into

$$\mathcal{B} = \begin{bmatrix} \mathcal{B}_{ll} & \mathcal{B}_{lf} \\ \mathcal{B}_{fl} & \mathcal{B}_{ff} \end{bmatrix}$$

with $\mathcal{B}_{ll} \in \mathbb{R}^{dl\times dl}, \mathcal{B}_{lf} \in \mathbb{R}^{dl\times df}, \mathcal{B}_{fl} \in \mathbb{R}^{dl\times df}$, and $\mathcal{B}_{ff} \in \mathbb{R}^{df\times df}$.

To propose the main technical result, it is still necessary to provide a definition concerning the unique target localization.

Definition 3 (*Unique Target Localization* [35]). The desired target localization $(G, p^*(t))$ is *unique* if $\mathcal{B}_{ff}$ in the bearing Laplacian $\mathcal{B}$ is nonsingular.

With the above definitions, it is ready to propose the main technical problem addressed by this paper.

Problem 1 (Event-triggered bearing-based localization): With the given anchors leaders (i.e., $u_i = 0, i \in \mathbb{I}_l$), design a coordinative event-triggered control signal

$$u_i(t) = \omega(g_{i,j}(t_s)), t \in [t_s, t_{s+1}], i \in \mathbb{I}_f, j \in \mathcal{N}_i,$$

for the followers in MAS governed by (1) and $G(\nu, \varepsilon)$ to achieve a unique localization given in Definition 3. Here, $s = 0, 1, 2, \cdots$, are the discrete event-triggering time constants. The triggering time sequences $t_s, s = 0, 1, 2, \ldots$, are calculated with a trigger function $f(\cdot)$ designed afterwards.

Remark 1 Distinct from previous time-driven bearing-only control methods [27–35] and event-triggered position-based control strategies [37–42], Problem 1 considers both natural nonlinear bounded bearing values (i.e., $\|g_{i,j}\| \leqslant 1$ in Eq. (7)) and event-triggered techniques for technical issues, which brings challenges in controller design, stability analysis and Zeno exclusion.

3 Main results

In this section, the event-triggered bearing-only localization control scheme is proposed with a guaranteed Zeno-free feature. Before presenting the main technical results, it is necessary to introduce some preliminaries.

Assumption 1 For an n-agent MAS with communication topology $G(\nu, \epsilon)$, it is assumed that the target localization (G, p^*) in Definition 3 is unique.

Assumption 1 guarantees the uniqueness of the final localization via bearing-only measurements.

Lemma 1 [35] Suppose no agents coincide in desired localization p^* or during the localization forming process, one has

$$\begin{aligned} p^{\mathsf{T}}\bar{H}^{\mathsf{T}}(g-g^*) \geqslant& \frac{\lambda_{\min}(\mathcal{B}_{ff})\|\delta_p\|^2}{2\|\bar{H}\|(\|\delta_p\|+\|\widetilde{p}^*\|)}, \\ (p^*)^{\mathsf{T}}\bar{H}^{\mathsf{T}}(g-g^*) \leqslant& 0, \\ (p-p^*)^{\mathsf{T}}\bar{H}^{\mathsf{T}}(g-g^*) \geqslant& 0, \end{aligned} \quad (11)$$

where all the three equalities hold if and only if $g = g^*$. Here, $g^* := [(g_1^*)^{\mathsf{T}}, (g_2^*)^{\mathsf{T}}, \ldots, (g_m^*)^{\mathsf{T}}]^{\mathsf{T}}$ denotes the desirable bearing vectors, $\delta_p := p - p^*$ is the errors between the position of agents and desired localization, and $\widetilde{p}^* := p^* - \mathbf{1}_n \otimes \bar{p}^*$ the unique geometric pattern of the localization with $\bar{p}^* := \sum_{i=1}^n p_i^*/n$ being a constant.

Remark 2 Due to the anchors or stationary leaders (i.e., $u_i = 0, i \in \mathbb{I}_l$) and the unique target localization in Definition 3, it can be deduced that the desired position p^* is stationary, which implies that the center of all the desired positions $\bar{p}^*$ keeps stationary as well (i.e., a constant) in Lemma 1.

Assumption 2 [35] Under Assumption 1, it is assumed that the initial values of position errors δ_p in (11) satisfy

$$\|\delta_p(0)\| \leqslant \frac{1}{\sqrt{n}}(\min_{i,j\in\nu}\|p_i^* - p_j^*\| - \beta)$$

with $\beta > 0$ being a positive constant.

Assumption 2 is a sufficient condition for initial noncoincidence of agents, which is indispensable for the exclusion of the Zeno behavior afterwards.

Analogously, in accordance to the stationary anchor leaders i.e., $p_i(t) = p_i(0),\ i \in \mathbb{I}_l, \forall t > 0$ in Problem 1, the proposed event-triggered control law $u_i, i \in \mathbb{I}_f$, is formulated as,

$$u_i(t) = \sum_{j\in\mathcal{N}_i} \gamma_i(g_{i,j}(t_s) - g_{i,j}^*), t \in [t_s, t_{s+1}], \quad (12)$$

where $\gamma_i \in \mathbb{R}^+, i \in \mathbb{I}_f$, is the control gain, and $s = 0, 1, 2, \cdots$, are the discrete event-triggering time constants. The triggering time sequences $t_s, s = 0, 1, 2, \ldots$, are designed as

$$t_{s+1} = \inf\Big\{t | t \geqslant t_s + \tau \text{ and } f(r, \delta_p) = 0\Big\}, \quad (13)$$

where $\tau \in \mathbb{R}^+$ is the threshold and

$$f(r, \delta_p) := \|r\| - \frac{\sigma\lambda_{\min}(\mathcal{B}_{ff})\|\delta_p\|}{2\|\bar{H}\|^2(\|\delta_p\| + \|\widetilde{p}^*\|)}, \quad (14)$$

where $\sigma \in (0, 1)$, $\bar{H}, \widetilde{p}^*, \delta_p$ are given in Eqs. (10), (11) and $r(t) := g(t_s) - g(t)$ denotes the bearing measurement errors for $t \in [t_s, t_{s+1}]$.

Now, the main technical result concerning Problem 1 is provided as below.

Theorem 1 For the leader-follower MAS governed by Eqs. (1), (12), and (14), Problem 1 is solved under Assumptions 1, 2. Moreover, the inter-event times satisfy $t_{s+1} - t_s \geqslant \tau$ with $\tau \in \mathbb{R}^+$ being the threshold.

Proof: See Appendix.

Remark 3 In the previous event-triggered control strategies [37–42] of the revised version, the input is generally designed based on the relative position, which implies that at least two kinds of sensors are required (distance measurement and bearing angle measurement) with high cost. However, the proposed controller in (12) is designed based on bearing-only information, which could measure bearings via only low-cost pin-hole cameras or wireless sensor arrays, and is hence more applicable in practice. Moreover, since the relative bearing is nonlinear and bounded, it brings challenging issues in the convergence analysis and exclusion of Zeno behavior when combining it with event-triggered technique.

4 Numerical simulation

In this section, we consider two kinds of localizations to validate the feasibility of Theorem 1. One is a 3-D localization, another is a sophisticated localization in a 2-D configuration space.

For a 3-D localization scenario, we consider a leader-follower MAS consisting of 2 leaders and 10 followers, whose inter-agent interaction topology G of the MAS is illustrated in Fig. 1 (a) under Assumption 1. Moreover, with an arbitrary oriented graph of the topology G, the target localization is set with the constant bearing g^* and prescribed relative distance, as shown in Fig. 1 (a). The initial positions of the leader-follower MAS are set as $p_1(0) = [4, 4, 4]^{\mathsf{T}}, p_2(0) = [4, 2, 4]^{\mathsf{T}}, p_3(0) = [-8, -9, -2]^{\mathsf{T}}, p_4(0) = [-7, -5, -3]^{\mathsf{T}}, p_5(0) = [2, -8, 3]^{\mathsf{T}}, p_6(0) = [-7, -3, 1]^{\mathsf{T}}, p_7(0) = [4, -8, 3]^{\mathsf{T}}, p_8(0) = [-7, -7, -4]^{\mathsf{T}}, p_9(0) = [-6, -7, -8]^{\mathsf{T}}, p_{10}(0) = [-7, -2, -4]^{\mathsf{T}}, p_{11}(0) = [-4, 4, 5]^{\mathsf{T}}$,

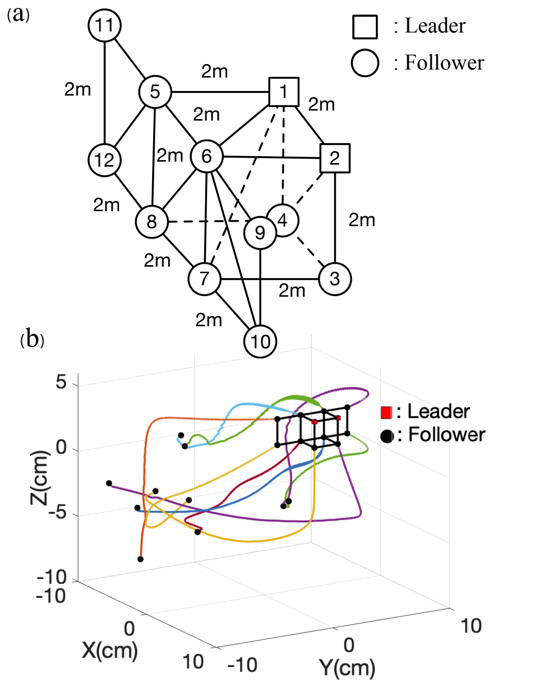

Fig. 1 (a) MAS topology and prescribed target localization of the leader-follow MAS. Here, agents $1-2$ are the leaders, agents $3-12$ the followers. (b) Trajectories of the event-triggered bearing-only unique target localization in a 3-D localization. Here, the red rectangles denote the leaders and the black circles the followers.

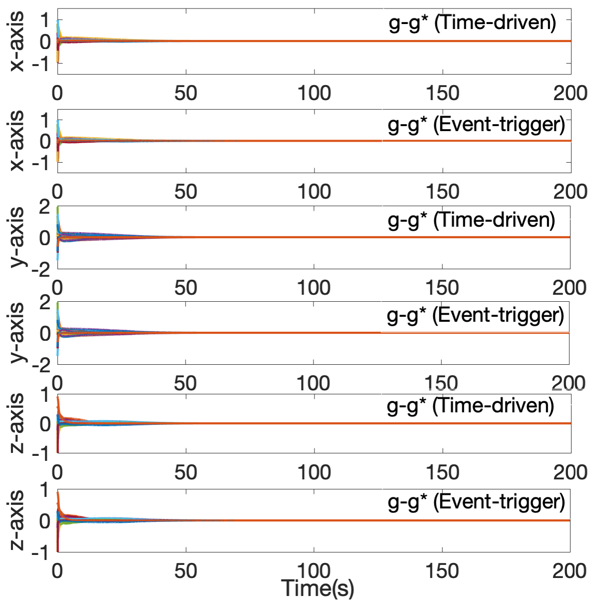

Fig. 2 Temporal evolution of the bearing vector errors $g-g^*$ in 3-D localization.

$p_{12}(0) = [-3, 4, -4]^{\mathsf{T}}$ with Assumption 2. In accordance to Theorem 1, the parameters for controller (12) are set as $\gamma_i = 10, i \in \mathbb{I}_f$ and σ in Eq. (20) is set as 0.5 satisfying $0 < \sigma < 1$.

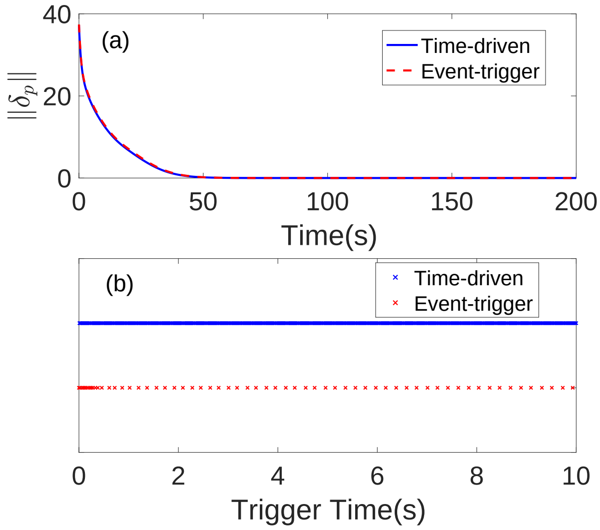

Fig. 3 (a) Temporal evolution of position errors norm $\|\delta_p\|$ in 3-D localization. (b) The discrete event-triggered time instants in 3-D localization. Specifically, there exists lower bound $\tau = 0.02s$ for triggering-time intervals in the 3-D localization.

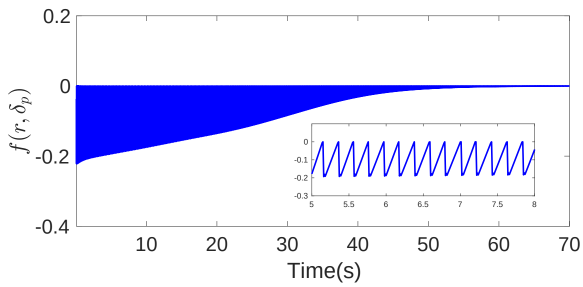

Fig. 4 Temporal evolution of the triggering function $f(r, \delta_p)$ in 3-D localization.

The trajectories of the event-triggered bearing-only localization illustrated in Fig. 1 (b), where the black circles denote the positions of followers and the red rectangles the positions of leaders. It is observed that the prescribed target 3-D localization is finally achieved by the followers in Fig. 1 (b). Compared with the time-driven bearing localization method [35], the evolution of bearing vector errors $g-g^*$ in Fig. 2 converge to zeros as well and hence the prescribed target localization is finally achieved, which substantiates the feasibility of Theorem 1. As shown in Fig. 3 (a), with substantial reduction of the calculation, sampling and communication cost, there is nearly no control performance degradation of the tracking errors $\|\delta_p\|$, which still converge asymptotically with the event-triggered controller. Moreover, as shown in Fig. 3 (b), the temporal evolution of the event-triggered times $t_{s+1} - t_s$ implies that there exists a minimum inter-event time interval of $\tau = 0.02$s, which further verifies the feasibility and effectiveness of the control scheme (12) and Theorem 1. Fig. 4 depicts the event-triggered phenomenon by the switching of the trigger function $f(r, \delta_p)$.

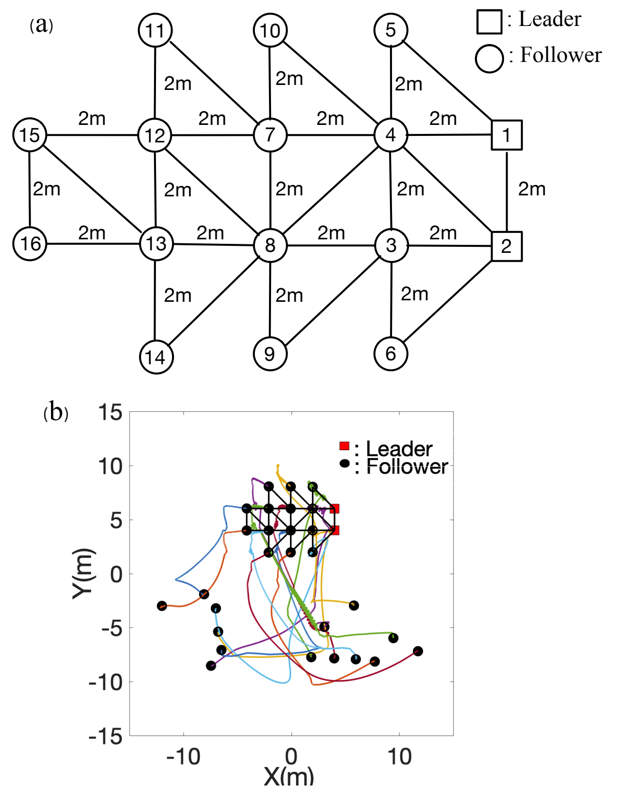

Fig. 5 (a) MAS topology and prescribed target localization of the leader-follow MAS. Here, agents $1-2$ are the leaders and agents $3-16$ are the followers. (b) Trajectories of the event-triggered bearing-only unique target localization in a 2-D localization. Here, the red rectangles denote the leaders and the black circles the followers.

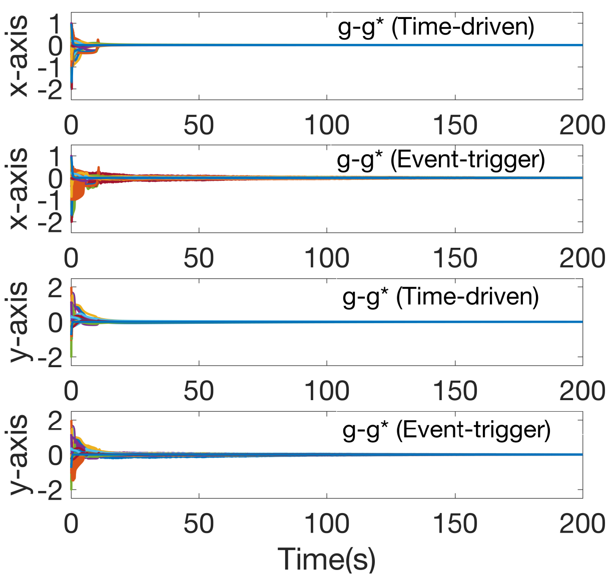

Fig. 6 Temporal evolution of the bearing vector errors $g-g^*$ in 2-D localization.

For the scenario of 2-D localization case, we consider a leader-follower MAS consisting of 2 leaders and 14 followers, whose inter-agent interaction topology G

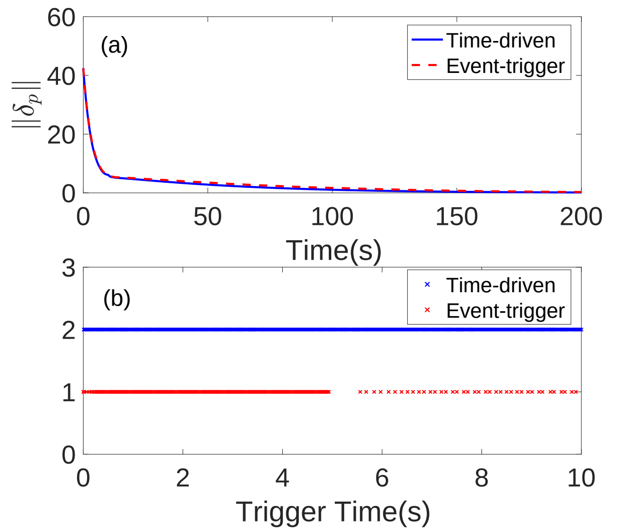

Fig. 7 (a) Temporal evolution of position errors norm $\|\delta_p\|$ in 2-D localization. (b) The discrete event-triggered time instants in 2-D localization. Specifically, there exists lower bound $\tau = 0.02s$ for triggering-time intervals.

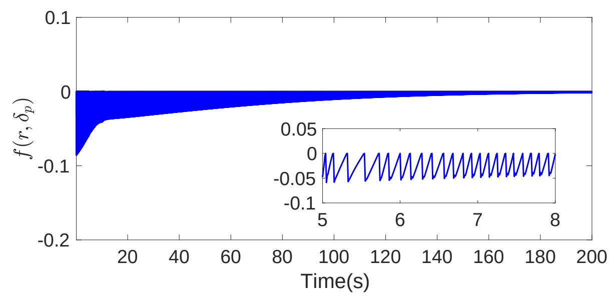

Fig. 8 Temporal evolution of the triggering function $f(r,\delta_p)$ in 2-D localization.

of the MAS is illustrated in Fig. 5 (a) under Assumption 1. Meanwhile, the target localization is set with the constant bearing g^* and prescribed relative distance, as shown in Fig. 5 (a) as well. The initial positions of the leader-follower MAS are set as $p_1(0) = [4,6]^\mathsf{T}, p_2(0) = [4,4]^\mathsf{T}, p_3(0) = [-8,-9]^\mathsf{T}, p_4(0) = [7,-5]^\mathsf{T}, p_5(0) = [2,-8]^\mathsf{T}, p_6(0) = [-7,-3]^\mathsf{T}, p_7(0) = [4,-8]^\mathsf{T}, p_8(0) = [-7,-7]^\mathsf{T}, p_9(0) = [8,-8]^\mathsf{T}, p_{10}(0) = [6,-3]^\mathsf{T}, p_{11}(0) = [3,-5]^\mathsf{T}, p_{12}(0) = [10,-6]^\mathsf{T}, p_{13}(0) = [6,-8]^\mathsf{T}, p_{14}(0) = [12,-7]^\mathsf{T}, p_{15}(0) = [-8,-2]^\mathsf{T}, p_{16}(0) = [-12,-3]^\mathsf{T}$ with Assumption 2. The parameters $\gamma_i = 10, i \in \mathbb{I}_f$ and σ in Eq. (20) for controller (12) are the same as the 3-D case.

Analogously, the trajectories of the event-triggered bearing-only localization are illustrated in Fig. 5 (b). It is observed that the prescribed target localization is finally achieved by the followers as well. The evolution of bearing vector errors $g-g^*$ in Fig. 6 converge to zeros as well, which implies that the prescribed target localization is finally achieved. As shown in Fig. 7 (a), the tracking errors $\|\delta_p\|$ still converge asymptotically with event-triggered controller, which is similar to Fig. 4 (a). Moreover, as shown in Fig. 7 (b), the temporal evolution of the event-triggered times $t_{s+1} - t_s$ clearly imply that there exists a minimum inter-event time interval of $\tau = 0.02$s, which verifies the feasibility and effectiveness of the control scheme (12) and Theorem 1 as well. In Fig. 8, it is observed that the event-triggered phenomenon implicitly exists by the switching of the trigger function $f(r, \delta_p)$.

5 Conclusion

In this paper, we propose an event-triggered bearing-only localization method for networked MASs. With such a localization protocol, the entire group forms a prescribed localization merely according to event-based bearing-only measurements in arbitrary dimension. Essentially, the conditions are derived guaranteeing both the asymptotical stability of the proposed protocol and the exclusion of Zeno behavior. Numerical simulations are conducted to substantiate the effectiveness of the proposed method. Such an event-based bearing-only method has application potential in collective patrolling, reconnaissance, resource explorations, environmental monitoring, etc., with abundant industrial multiple unmanned systems, mobile robots and vehicles.

References:

[1] CHEN Z, ZHANG H T. No-beacon collective circular motion of jointly connected multi-agents.*Automatica*, 2011, 47: 1929–1937.

[2] ZHANG H T, CHEN Z, YAN L, et al. Applications of collective circular motion control to multirobot systems. *IEEE Transactions on Control Systems Technology*, 2012, 21(4): 1416–1422.

[3] LIU B, CHEN Z, ZHANG H T, et al. Collective dynamics and control for multiple unmanned surface vessels. *IEEE Transactions on Control Systems Technology*, 2020, 28(6): 2540–2547.

[4] Zhang H T, Hu B B, Xu Z, et al. Visual Navigation and Landing Control of an Unmanned Aerial Vehicle on a Moving Autonomous Surface Vehicle via Adaptive Learning.*IEEE Transactions on Neural Networks and Learning Systems*, 2021, in press, doi: 10.1109/TNNLS.2021.3080980.

[5] PENG Z, WANG J. Output-feedback path-following control of autonomous underwater vehicles based on an extended state observer and projection neural networks. *IEEE Transactions on Systems, Man, and Cybernetics: Systems*, 2017, 48(4): 535–544.

[6] HONG Y, HU J, GAO L. Tracking control for multi-agent consensus with an active leader and variable topology. *Automatica*, 2006, 42(7): 1177–1182.

[7] Yao W, de Marina H G, Lin B, et al. Singularity-free guiding vector field for robot navigation. *IEEE Transactions on Robotics*, 2021, in press, doi:10.1109/TRO.2020.3043690.

[8] Su H, Long M, Zeng Z. Controllability of two-time-scale discrete-time multiagent systems.*IEEE transactions on cybernetics*, 2018, 50(4): 1440-1449.

[9] Long M, Su H, Zeng Z. Model-Free Event-Triggered Consensus Algorithm for Multiagent Systems Using Reinforcement Learning Method. IEEE Transactions on Systems, Man, and Cybernetics: Systems, 2021, in press: 10.1109/TSMC.2021.3120008.

[10] NI W, CHENG D. Leader-following consensus of multi-agent systems under fixed and switching topologies. *Systems & Control Letters*, 2010. 59(3-4): 209–217.

[11] HU B B, ZHANG H T, WANG J. Multiple-target surrounding and collision avoidance with second-order nonlinear multi-agent systems. *IEEE Transactions on Industrial Electronics*, 2020, in press, doi:10.1109/TIE.2020.3000092.

[12] Kou L, Huang Y, Chen Z, et al. Cooperative fencing control of multiple second-order vehicles for a moving target with and without velocity measurements. *International Journal of Robust and Nonlinear Control*, 2021, 31(10): 4602-4615.

[13] HU B B, ZHANG H T, LIU B, et al. Distributed Surrounding Control of Multiple Unmanned Surface Vessels with Varying Interconnection Topologies. *IEEE Transactions on Control Systems Technology*, 2021, in press, doi:10.1109/TCST.2021.3057640.

[14] HU B B, CHEN Z. ZHANG H T. Distributed Moving Target Fencing in a Regular Polygon Formation. *IEEE Transactions on Control of Network System*, 2021, in press, doi:10.1109/TCNS.2021.3094784.

[15] LIN Z, FU M, DIAO Y. Distributed self localization for relative position sensing networks in 2D space. *IEEE Transactions on Signal Processing*, 2015, 63(4): 3751 – 3761.

[16] Jafari S, Ajorlou A, Aghdam A G. Leader localization in multi-agent systems subject to failure: A graph-theoretic approach. *Automatica*, 2011, 47(8): 1744-1750.

[17] Shames I, Fidan B, Anderson B D O. Minimization of the effect of noisy measurements on localization of multi-agent autonomous formations.*Automatica*, 2009, 45(4): 1058-1065.

[18] ASPNES J, EREN T, GOLDENBERG D K, et al. A theory of network localization. *IEEE Transactions on Mobile Computing*, 2006, 12(5): 1663 – 1678.

[19] DIAO Y, LIN Z, FU M. A barycentric coordinate based distributed localization algorithm for sensor networks. *IEEE Transactions on Signal Processing*, 2014, 62(18): 4760 – 4771.

[20] KHAN U A, KAR S, MOURA J M F. Distributed sensor localization in random environments using minimal number of anchor nodes. *IEEE Transactions on Signal Processing*, 2009, 57(5): 2000 – 2016.

[21] MAO G, FIDAN B, ANDERSON, B. D. O. Wireless sensor network localization techniques. *Comupter Networks*, 2007, 51: 2529 – 2553.

[22] BISHOP A N, ANDERSON B D O, FIDAN B, et al. Bearing-only localization using geometrically constrained optimization. *IEEE Transactions on Aerospace and Electronic Systems*, 2009, 45(1): 308 – 320.

[23] PIOCAN G, SHAMES I, FIDAN B, et al. On frame and orientation localization for relative sensing networks. *Automatica*, 2013, 49: 206 – 213.

[24] SHAMES I, BISHOP A N, ANDERSON B D O. Analysis of noisy bearing-only network localization. *IEEE Transactions on Automatic Control*, 2013, 58: 247 – 252.

[25] HU B B, ZHANG H T. Bearing-only Motional Target-Surrounding Control for Multiple Unmanned Surface Vessels. *IEEE Transactions on Industrial Electronics*, 2021, in press, doi: 10.1109/TIE.2021.3076719.

[26] ZHU G, HU J. A distributed continuous-time algorithm for network localization using angle-of-arrival information. *Automatica*, 2014, 50: 53 – 63.

[27] BASIRI M, BISHOP A N, JENSFELT P. Distributed control of triangular formations with angle-only constraints. *Systems & Control Letters*, 2010, 59(2): 147–154.

[28] ZHAO S, LIN F, PENG K, et al. Distributed control of angle-constrained cyclic formations using bearing-only measurements. *Systems & Control Letters*, 2014, 63: 12–24.

[29] EREN, T. Formation shape control based on bearing rigidity. *International Journal of Control*, 2012, 85(9): 1361–1379.

[30] FRANCHI A, GIORDANO P R. Decentralized control of parallel rigid formations with direction constraints and bearing measurements.*Proceedings of IEEE Conference on Decision & Control*, Maui: IEEE, 2012: 5310-5317.

[31] ZHAO S. ZELAZO, D. Bearing rigidity and almost global bearing-only formation stabilization. *IEEE Transactions on Automatic Control*, 2016 , 61(5): 1255–1268.

[32] ZHAO S, ZELAZO D. Translational and scaling formation maneuver control via a bearing-based approach. *IEEE Transactions on Control of Network Systems*, 2015, 4(3): 429–438.

[33] TRON R, THOMAS J, LOIANNO G, et al. Bearing-only formation control with auxiliary distance measurements, leaders, and collision avoidance. *Proceedins of IEEE Conference on Decision and Control*, Las Vegas: IEEE, 2016: 1806–1813.

[34] ZHAO S, ZELAZO D. Localizability and distributed protocols for bearing-based network localization in arbitrary dimensions. *Automatica*, 2016, 69: 334–341.

[35] ZHAO S, LI Z, DING Z. Bearing-only formation tracking control of multiagent systems. *IEEE Transactions on Automatic Control*, 2019, 64(11): 4541–4554.

[36] CHEN Z, HAN Q L, YAN Y, et al. How often should one update control and estimation: review of networked triggering techniques. *Science China Information Sciences*, 2020, 63(5): 150201.

[37] MENG X, CHEN T. Event based agreement protocols for multi-agent networks. *Automatica*, 2013, 49(7): 2125–2132.

[38] GUO G, DING L, HAN Q L. A distributed event-triggered transmission strategy for sampled-data consensus of multi-agent systems. *Automatica*, 2014, 50(5): 1489–1496.

[39] MENG H, ZHANG H T, WANG Z, et al. Event-triggered control for semiglobal robust consensus of a class of nonlinear uncertain multiagent systems. *IEEE Transactions on Automatic Control*, 2019, 65(4): 1683–1690.

[40] ZHU W, JIANG Z, FENG G. Event-based consensus of multi-agent systems with general linear models. *Automatica*, 2014, 50(2): 552–558.

[41] LI H, LIAO X, HUANG T, et al. Event-triggering sampling based leader-following consensus in second-order multi-agent systems.*IEEE Transactions on Automatic Control*, 2015, 60(7): 1998–2003.

[42] HUANG N, DUAN Z, WEN G, et al. Event-triggered consensus tracking of multi-agent systems with lur'e nonlinear dynamics. *International Journal of Control*, 2016, 89(5): 1025–1037.

[43] GODSIL C, ROYLE G F. *Algebraic Graph Theory*. New York: Springer Science & Business Media, 2013.

[44] KHAIL H K, GRIZZLE J W. *Nonlinear Systems*. Upper Saddle River: Prentice Hall, 2002.

Appendix Proof of Theorem 1

The proof consists of two claims, where the convergence of bearing-based localization and exclusion of the Zeno behavior are proved sequentially.

Claim 1: Convergence of bearing-based localization.

With the assistance of the incidence matrix $\bar{H}$ in Eq. (9), rewrite the controller (12) in a compact form as

$$u(t) = -\begin{bmatrix} 0 & 0 \\ 0 & I_{df} \end{bmatrix} \bar{H}^{\mathsf{T}} \Gamma_1 (g(t_s) - g^*), \tag{15}$$

with $g(t_s) := [g_1(t_s)^{\mathsf{T}}, g_2(t_s)^{\mathsf{T}}, \ldots, g_m(t_s)^{\mathsf{T}}]^{\mathsf{T}}$, $\Gamma_1 = \mathrm{diag}\{\gamma_i \otimes I_d\} \in \mathbb{R}^{nd \times nd}$ a positive definite matrix and $I_{df} \in \mathbb{R}^{df \times df}$ an identity matrix.

Rewrite $\delta_p = [\delta_l^{\mathsf{T}}, \delta_f^{\mathsf{T}}]^{\mathsf{T}}$ with $\delta_l := p_l - p_l^*, \delta_f := p_f - p_f^*$ as the position errors of the leaders and the followers, respectively. Here, $p_l = [p_1^{\mathsf{T}}, p_2^{\mathsf{T}}, \ldots, p_l^{\mathsf{T}}]^{\mathsf{T}}, p_l^* = [(p_1^*)^{\mathsf{T}}, (p_2*)^{\mathsf{T}}, \ldots, (p_l^*)^{\mathsf{T}}]^{\mathsf{T}}, p_f = [p_{l+1}^{\mathsf{T}}, p_{l+2}^{\mathsf{T}}, \ldots, p_n^{\mathsf{T}}]^{\mathsf{T}}, p_f^* = [(p_{l+1}^*)^{\mathsf{T}}, (p_{l+2}^*)^{\mathsf{T}}, \ldots, (p_n^*)^{\mathsf{T}}]^{\mathsf{T}}$ are the positions and desired positions of the leaders and followers, respectively.

From the fact of stationary anchor leaders, one has $\delta_l = 0$, which implies that

$$\delta_p^{\mathsf{T}} \times \begin{bmatrix} 0 & 0 \\ 0 & I_{df} \end{bmatrix} = [\delta_l^{\mathsf{T}}, \delta_f^{\mathsf{T}}] \times \begin{bmatrix} 0 & 0 \\ 0 & I_{df} \end{bmatrix} = \delta_p^{\mathsf{T}}. \tag{16}$$

Then, taking temporal derivative of δ_p in (11) and considering Eqs. (1) and (15), one has the dynamic of δ_p as

$$\dot{\delta}_p = u = -\begin{bmatrix} 0 & 0 \\ 0 & I_{df} \end{bmatrix} \bar{H}^{\mathsf{T}} \Gamma_1 (g(t_s) - g^*). \tag{17}$$

Let $r(t) := g(t_s) - g(t)$ be the bearing measurement errors for $t \in [t_s, t_{s+1}]$. For neatness, denote $r = r(t)$ and $g = g(t)$, and one has

$$\dot{\delta}_p = -\begin{bmatrix} 0 & 0 \\ 0 & I_{df} \end{bmatrix} \bar{H}^{\mathsf{T}} \Gamma_1 (g - g^* + r). \tag{18}$$

Pick a Lyapunov candidate as $V(\delta_p) = 1/2\|\delta_p\|^2$, whose derivative along the trajectory of Eq. (18) is

$$\begin{aligned} \dot{V}(\delta_p) =& \delta_p^{\mathsf{T}} \dot{\delta}_p \\ =& -\delta_p^{\mathsf{T}} \begin{bmatrix} 0 & 0 \\ 0 & I_{df} \end{bmatrix} \bar{H}^{\mathsf{T}} (g - g^* + r) \\ =& -\delta_p^{\mathsf{T}} \bar{H}^{\mathsf{T}} (g - g^* + r) \\ =& -\delta_p^{\mathsf{T}} \bar{H}^{\mathsf{T}} \Gamma_1 (g - g^*) - \delta_p^{\mathsf{T}} \bar{H}^{\mathsf{T}} \Gamma_1 r. \end{aligned} \tag{19}$$

It follows from Lemma 1 and Eq. (19) that

$$\begin{aligned} \dot{V}(\delta_p) \leqslant& -\frac{\lambda_{\min}(\mathcal{B}_{ff})\|\delta_p\|^2 \cdot \|\Gamma_1\|}{2\|\bar{H}\|(\|\delta_p\| + \|\widetilde{p}^*\|)} \\ &+ \|\delta_p\| \cdot \|\bar{H}\| \cdot \|\Gamma_1\| \cdot \|r\| \\ \leqslant& -(1-\sigma)\frac{\lambda_{\min}(\mathcal{B}_{ff})\|\delta_p\|^2 \cdot \|\Gamma_1\|}{2\|\bar{H}\|(\|\delta_p\| + \|\widetilde{p}^*\|)} \\ &- \sigma \frac{\lambda_{\min}(\mathcal{B}_{ff})\|\delta_p\|^2 \cdot \|\Gamma_1\|}{2\|\bar{H}\|(\|\delta_p\| + \|\widetilde{p}^*\|)} \\ &+ \|\delta_p\| \cdot \|\bar{H}\| \cdot \|\Gamma_1\| \cdot \|r\| \\ \leqslant& -(1-\sigma)\frac{\lambda_{\min}(\mathcal{B}_{ff})\|\delta_p\|^2 \cdot \|\Gamma_1\|}{2\|\bar{H}\|(\|\delta_p\| + \|\widetilde{p}^*\|)} \\ &+ \|\delta_p\| \cdot \Bigg(\|\bar{H}\| \cdot \|\Gamma_1\| \cdot \|r\| \\ &- \frac{\sigma\lambda_{\min}(\mathcal{B}_{ff})\|\delta_p\|| \cdot \|\Gamma_1\|}{2\|\bar{H}\|(\|\delta_p\| + \|\widetilde{p}^*\|)} \Bigg) \end{aligned}$$

with $\|\Gamma_1\| > 0$, $\|\bar{H}\| > 0$ and $0 < \sigma < 1$. Let r satisfy

$$\|r\| \leqslant \frac{\sigma\lambda_{\min}(\mathcal{B}_{ff})\|\delta_p\|}{2\|\bar{H}^2\|(\|\delta_p\| + \|\widetilde{p}^*\|)}, \tag{20}$$

one has

$$\dot{V}(\delta_p) \leqslant -(1-\sigma)\frac{\lambda_{\min}(\mathcal{B}_{ff})\|\Gamma_1\| \cdot \|\delta_p\|^2}{2\|\bar{H}\|(\|\delta_p\| + \|\widetilde{p}^*\|)} \leqslant 0, \tag{21}$$

which is strictly negative if $\|\delta_p\| \neq 0$. Then, it derives that $V(\delta_p)$ converges when $\|\delta_p\| \neq 0$. Moreover, $\dot{V}(\delta_p) = 0$ if and only if $\|\delta_p\| = 0$, equivalently, $\delta_p = 0$ is the only stable equilibrium point of the closed-loop system (18). Accordingly, the closed-loop system δ_p is input-to-state stable (ISS) [44], which implies that $\lim_{t\to\infty} \|\delta_p(t)\| = 0$. Moreover, note that the triggered condition $f(r, \delta_p)$ could be derived as in Eq. (14).

Claim 2: Zeno exclusion.

This claim is equivalent to prove that the inter-event times $t_{s+1} - t_s$ are with a lower-bounded strictly positive time interval, which is triggered when $f(r, \delta_p) = 0$, i.e.,

$$\frac{\|r\| \cdot (\|\delta_p\| + \|\widetilde{p}^*\|)}{\|\delta_p\|} = \frac{\sigma\lambda_{\min}(\mathcal{B}_{ff})}{2\|\bar{H}\|^2}. \tag{22}$$

To calculate the sophisticated derivative of $\|r\| + \|r\| \cdot \|\widetilde{p}^*\|/\|\delta_p\|$ in Eq. (22), we first compute the temporal derivative of $\|r\|$ and $\|r\|/\|\delta_p\|$, respectively,

$$\frac{d}{dt}\|r\| = \frac{d}{dt}(r^{\mathsf{T}}r)^{\frac{1}{2}} = \frac{r^{\mathsf{T}}\dot{r}}{\|r\|} = -\frac{r^{\mathsf{T}}\dot{g}}{\|r\|}.$$

It follows from Eq. (10) that

$$\begin{aligned}\frac{d}{dt}\|r\| =& -\frac{r^{\mathsf{T}}\mathrm{diag}\left(\frac{\mathrm{P}_{\mathrm{g_k}}}{\|\mathrm{e_k}\|}\right)\bar{\mathrm{H}}\dot{\delta}_{\mathrm{p}}}{\|r\|} \\ \leqslant& \frac{\|r\| \cdot \left\|\mathrm{diag}\left(\frac{\mathrm{P}_{\mathrm{g_k}}}{\|\mathrm{e_k}\|}\right)\right\| \cdot \|\bar{\mathrm{H}}\| \cdot \|\dot{\delta}_{\mathrm{p}}\|}{\|r\|} \\ \leqslant& \left\|\mathrm{diag}\left(\frac{\mathrm{P}_{\mathrm{g_k}}}{\|\mathrm{e_k}\|}\right)\right\| \cdot \|\bar{\mathrm{H}}\| \cdot \|\dot{\delta}_{\mathrm{p}}\|.\end{aligned}$$

In accordance to Assumption 2, one has

$$\begin{aligned}\|p_i - p_j\| =&(p_i - p_i^*) - (p_j - p_j^*) + (p_i^* - p_j^*) \\ \geqslant& \|p_i^* - p_j^*\| - \|p_i(t) - p_i^*\| - \|p_j(t) - p_j^*\| \\ \geqslant& \|p_i^* - p_j^*\| - \sum_{k=1}^{n}\|p_k(t) - p_k^*(t)\| \\ \geqslant& \|p_i^* - p_j^*\| - \sqrt{n}\|\delta_p(t)\|\end{aligned}$$

for $\forall i, j \in \nu$. Since $\dot{V}(t) \leqslant 0$ given in Eq. (21), one has $\|\delta_p(t)\| \leqslant \delta_p(0)$ for $t \geqslant 0$, which implies that

$$\|p_i(t) - p_j(t)\| \geqslant \|p_i^* - p_j^*\| - \sqrt{n}\|\delta_p(0)\| \geqslant \beta. \tag{23}$$

Then, it implicitly implies the noncoincidence among any two agents i, j is achieved. As $\|P_{g_k}\| \leqslant 1, \|g - g^*\| \leqslant 2m$, it then follows from Eqs. (18) and (23) that

$$\begin{aligned}\frac{d}{dt}\|r\| \leqslant& \frac{1}{\beta}\|\bar{H}\| \cdot \left\| \begin{bmatrix} 0 & 0 \\ 0 & I_{df}\end{bmatrix} \bar{H}^{\mathsf{T}}(g(t_s) - g^*)\right\| \\ \leqslant& \frac{1}{\beta}\|\bar{H}\| \cdot \left\| \begin{bmatrix} 0 & 0 \\ 0 & I_{df}\end{bmatrix} \right\| \cdot \|\bar{H}^{\mathsf{T}}\| \cdot \|(g(t) - g^* + r)\| \\ \leqslant& \frac{1}{\beta}\|\bar{H}\| \cdot \ \|\bar{H}^{\mathsf{T}}\| \cdot \|(g(t) - g^*)\| + \frac{1}{\beta}\|\bar{H}\| \cdot \|\bar{H}^{\mathsf{T}}\| \cdot \|r\| \\ \leqslant& \frac{2m}{\beta}\|\bar{H}\| \cdot \ \|\bar{H}^{\mathsf{T}}\| + \frac{1}{\beta}\|\bar{H}\| \cdot \|\bar{H}^{\mathsf{T}}\| \cdot \|r\| \\ \leqslant& 2m\alpha_1 + \alpha_1\|r\|\end{aligned} \tag{24}$$

with $\alpha_1 := \|\bar{H}\| \cdot \|\bar{H}^{\mathsf{T}}\|/\beta > 0$. Analogously, taking temporal derivative of $\|r\|/\|\delta_p\|$, one has

$$\begin{aligned}\frac{d}{dt}\frac{\|r\|}{\|\delta_p\|} =& \frac{\left(\frac{r^{\mathsf{T}}\dot{r}}{\|r\|} \cdot \|\delta_p\| - \|r\|\frac{\delta_p^{\mathsf{T}}\dot{\delta}_p}{\|\delta_p\|}\right)}{\|\delta_p\|^2} \\ \leqslant& \frac{\left(-\frac{r^{\mathsf{T}}\dot{g}}{\|r\|} \cdot \|\delta_p\| - \|r\|\frac{\delta_p^{\mathsf{T}}\dot{\delta}_p}{\|\delta_p\|}\right)}{\|\delta_p\|^2} \\ \leqslant& -\frac{\frac{r^{\mathsf{T}}\dot{g}}{\|r\|} \cdot \|\delta_p\|}{\|\delta_p\|^2} - \frac{\|r\|\frac{\delta_p^{\mathsf{T}}\dot{\delta}_p}{\|\delta_p\|}}{\|\delta_p\|^2} \\ \leqslant& \left(\left\|\mathrm{diag}\left(\frac{\mathrm{P}_{\mathrm{g_k}}}{\|\mathrm{e_k}\|}\right)\right\| \cdot \|\bar{\mathrm{H}}\| + \frac{\|\mathrm{r}\|}{\|\delta_{\mathrm{p}}\|}\right)\frac{\|\dot{\delta}_{\mathrm{p}}\|}{\|\delta_{\mathrm{p}}\|}.\end{aligned} \tag{25}$$

Substituting Eq. (18) into Eq. (25) yields

$$\begin{aligned}\frac{d}{dt}\frac{\|r\|}{\|\delta_p\|} \leqslant& \left(\left\|\mathrm{diag}\left(\frac{\mathrm{P}_{\mathrm{g_k}}}{\|\mathrm{e_k}\|}\right)\right\| \cdot \|\bar{\mathrm{H}}\| + \frac{\|\mathrm{r}\|}{\|\delta_{\mathrm{p}}\|}\right) \\ &\times \frac{\|(g(t) - g^* + r)\|}{\|\delta_p\|} \cdot \left\| \begin{bmatrix} 0 & 0 \\ 0 & I_{df}\end{bmatrix} \right\| \cdot \|\bar{H}^{\mathsf{T}}\| \\ \leqslant& \left(\frac{\|\bar{H}\|}{\beta} + \frac{\|r\|}{\|\delta_p\|}\right) \\ &\left(\frac{\|\bar{H}^{\mathsf{T}}\| \cdot \|(g(t) - g^*\|}{\|\delta_p\|} + \frac{\|\bar{H}^{\mathsf{T}}\| \cdot \|r\|}{\|\delta_p\|}\right).\end{aligned} \tag{26}$$

According to Lemma 1, one has

$$\delta_p^{\mathsf{T}}\bar{H}^{\mathsf{T}}(g - g^*) = (p - p^*)^{\mathsf{T}}\bar{H}^{\mathsf{T}}(g - g^*) \geqslant 0,$$

which implies that

$$\delta_p^{\mathsf{T}}\bar{H}^{\mathsf{T}}(g - g^*) \geqslant p^{\mathsf{T}}\bar{H}^{\mathsf{T}}(g - g^*) \geqslant \frac{\lambda_{\min}(\mathcal{B}_{ff})\|\delta_p\|^2}{2\|\bar{H}\|(\|\delta_p\| + \|\widetilde{p}^*\|)}.$$

Since $\delta_p(t) \leqslant \delta_p(0)$, it can be deduced that

$$\delta_p^{\mathsf{T}}\bar{H}^{\mathsf{T}}(g - g^*) \geqslant \frac{\lambda_{\min}(\mathcal{B}_{ff})\|\delta_p\|^2}{2\|\bar{H}\|(\|\delta_p(0)\| + \|\widetilde{p}^*\|)},$$

which immediately leads to

$$\begin{aligned}\frac{\|\bar{H}\| \cdot \|(g - g^*)\|}{\|\delta_p\|} \geqslant& \frac{\lambda_{\min}(\mathcal{B}_{ff})}{2\|\bar{H}\|(\|\delta_p(0)\| + \|\widetilde{p}^*\|)} \\ \geqslant& \frac{\sqrt{n}\lambda_{\min}(\mathcal{B}_{ff})}{2\|\bar{H}\|\kappa}\end{aligned}$$

with $\|\delta_p\| \neq 0$ and $\kappa = (\min_{i,j\in\nu}\|p_i^* - p_j^*\| - \beta) + \|\widetilde{p}^*\|)$. Thus, Eq. (26) can be converted into

$$\begin{aligned}\frac{d}{dt}\frac{\|r\|}{\|\delta_p\|} \leqslant& \left(\frac{\|\bar{H}\|}{\beta} + \frac{\|r\|}{\|\delta_p\|}\right) \\ &\times \left(\frac{\|\bar{H}^{\mathsf{T}}\| \cdot \|(g(t) - g^*\|}{\|\delta_p\|} + \frac{\|\bar{H}^{\mathsf{T}}\| \cdot \|r\|}{\|\delta_p\|}\right) \\ \leqslant& \|\bar{H}\|\left(\gamma_1 + \frac{\|r\|}{\|\delta_p\|}\right)^2\end{aligned} \tag{27}$$

for $\gamma_1 := \max\{(\sqrt{n}\lambda_{\min}(\mathcal{B}_{ff}))/(2\|\bar{H}\|^2\kappa),\ \|\bar{H}\|/\beta\} > 0$. Using the notation of $y_1 := \|r\|, y_2 := \|r\|/\|\delta_p\|$ for conciseness, it follows from Eqs. (24) and (27) that

$$\dot{y}_1 \leqslant \alpha_1(2 + y_1),\ \dot{y}_2 \leqslant \|\bar{H}\|(\gamma_1 + y_2)^2.$$

Accordingly,

$$\begin{aligned}&y_1(t) \leqslant \phi_1(t, \phi_1^0) = 2e^{\alpha_1 t} - 2, \\ &y_2(t) \leqslant \phi_2(t, \phi_2^0) = \frac{-1}{\|\bar{H}\|t + \gamma_1} - \gamma_1,\end{aligned} \tag{28}$$

where $\phi_1(t, \phi_1^0), \phi_2(t, \phi_2^0)$ are the solutions of

$$\begin{aligned}&\dot{\phi}_1 = \alpha_1(2 + \phi_1),\ \phi_1(0, \phi_1^0) = 0, \\ &\dot{\phi}_2 = \|\bar{H}\|(\gamma_1 + \phi_1)^2,\ \phi_2(0, \phi_2^0) = 0,\end{aligned}$$

which implies that

$$\frac{\|r\| \cdot (\|\delta_p\| + \|\widetilde{p}^*\|)}{\|\delta_p\|} = y_1(t) + \|\widetilde{p}^*\| \cdot y_2(t)$$

$$\leqslant \phi_1(t) + \|\widetilde{p}^*\| \cdot \phi_2(t).$$

Therefore, the inter-event time is $\{t_{s+1} - t_s\} \geqslant \tau$, which satisfies

$$\phi_1(\tau, 0) + \|\widetilde{p}^*\| \cdot \phi_2(\tau, 0) = \frac{\sigma \lambda_{\min}(\mathcal{B}_{ff})}{2\|\bar{H}\|^2}.$$

According to the monotonically increasing property of ϕ_1, ϕ_2 in Eq. (28), there exists a lower time boundary τ such that $\{t_{s+1} - t_s\} \geqslant \tau$ with a parameter $0 < \sigma < 1$. The proof is thus completed.

作者简介:

胡斌斌 博士研究生, 目前研究方向为多智能体协同理论与多无人艇应用, E-mail: hbb@hust.edu.cn;

张海涛 教授, 目前研究方向为群体智能，人工智能，自主无人艇集群协同控制, E-mail: zht@mail.hust.edu.cn.